

2009

Alignment Of Magnetic Anisotropy Axes In Crystals Of Mn₁₂ Acetate And Mn₁₂-tBuAc Molecular Nanomagnets: Angle-Dependent Ac Susceptibility Study

E Burzurí

Ch Carbonera

F Luis

D Ruiz-Molina

Christos Lampropoulos

University of North Florida, c.lampropoulos@unf.edu

See next page for additional authors

Follow this and additional works at: https://digitalcommons.unf.edu/achm_facpub

 Part of the [Chemistry Commons](#)

Recommended Citation

Burzurí, E; Carbonera, Ch; Luis, F; Ruiz-Molina, D; Lampropoulos, Christos; and Christou, G, "Alignment Of Magnetic Anisotropy Axes In Crystals Of Mn₁₂ Acetate And Mn₁₂-tBuAc Molecular Nanomagnets: Angle-Dependent Ac Susceptibility Study" (2009). *Chemistry Faculty Publications*. 13.
https://digitalcommons.unf.edu/achm_facpub/13

This Article is brought to you for free and open access by the Department of Chemistry at UNF Digital Commons. It has been accepted for inclusion in Chemistry Faculty Publications by an authorized administrator of UNF Digital Commons. For more information, please contact [Digital Projects](#).

© 2009 All Rights Reserved

Authors

E Burzurí, Ch Carbonera, F Luis, D Ruiz-Molina, Christos Lampropoulos, and G Christou

Alignment of magnetic anisotropy axes in crystals of Mn_{12} acetate and Mn_{12} -tBuAc molecular nanomagnets: Angle-dependent ac susceptibility study

E. Burzurí, Ch. Carbonera, and F. Luis*

Instituto de Ciencia de Materiales de Aragón, CSIC–Universidad de Zaragoza, 50009 Zaragoza, Spain

D. Ruiz-Molina

Centro de Investigación en Nanociencia y Nanotecnología (CIN2, CSIC-ICN), Campus UAB-Edifici CM7, 08193 Bellaterra, Spain

C. Lampropoulos and G. Christou

Department of Chemistry, University of Florida, Gainesville, Florida 32606, USA

(Received 15 September 2009; revised manuscript received 1 December 2009; published 31 December 2009)

We report the results of angular-dependent ac susceptibility experiments performed on two derivatives of Mn_{12} single-molecular magnets: the well-known Mn_{12} acetate, which contains disordered acetic acid molecules in interstitial sites of the crystal structure and Mn_{12} -tBuAc, for which solvent molecules are very well ordered in the structure. Our results show (a) that the angular variation is very similar in the two compounds investigated and compatible with a maximum misalignment of the anisotropy axes of less than 3° and (b) that the tunneling rate is faster for the better ordered Mn_{12} -tBuAc compound. These experiments question interstitial disorder as the dominant origin of the thermally activated tunneling phenomenon.

DOI: [10.1103/PhysRevB.80.224428](https://doi.org/10.1103/PhysRevB.80.224428)

PACS number(s): 75.45. j, 75.50.Xx, 75.60.Jk, 75.40.Gb

Molecular clusters such as Mn_{12} and Fe_8 are seen as the ultimate limit in the miniaturization of magnetic nanoparticles.¹ These clusters have a large spin ($S=10$ in Mn_{12}) and show magnetic hysteresis below liquid helium temperatures, much as larger nanoparticles do.^{2–4} The hysteresis phenomenon is caused by large magnetic anisotropy energy barriers $U \approx DS^2 \approx 70$ K, with D being an anisotropy parameter, which separate spin-up and spin-down states. In contrast to other nanostructured magnetic materials, single molecule magnets are monodisperse and tend to form crystals, therefore offering the possibility of investigating the physics of individual molecules with conventional experimental techniques.

Early studies revealed the existence of phenomena, such as quantum tunneling of the molecular spin,^{5–7} which are typical of the atomic world. Despite the intense research activity in this field, the origin of quantum tunneling in Mn_{12} remains somewhat obscure. In recent years, it has been suggested that the off-diagonal energy terms that induce quantum spin tunneling are caused mainly by small distortions of the molecular core.⁸ In some compounds, such as Mn_{12} acetate, distortions have been associated with disorder in the orientations of interstitial solvent molecules.⁹ Two major consequences would be a tilt of the anisotropy axes of the molecules from the crystalline c axis and the appearance of second-order off-diagonal terms $E(S_x^2 - S_y^2)$, forbidden by the fourfold symmetry of the undistorted molecular core. Tilts of the anisotropy axes of about 1.7° have been reported from high-field electron-spin resonance (ESR) experiments performed on Mn_{12} acetate¹⁰ and misalignments as high as 7° have been estimated from studies of the magnetic relaxation in the Mn_{12} -BrAc derivative.¹¹ However, later magnetization hysteresis¹² and magnetic neutron diffraction¹³ studies point to much smaller deviations from collinearity.

The aim of the present work is to study, by means of angular-dependent susceptibility experiments, the effect that

solvent disorder has on the orientation of the anisotropy axes and the quantum tunneling rates. We compare results obtained for two Mn_{12} derivatives: Mn_{12} acetate and Mn_{12} -tBuAc. In the latter, solvent molecules are extremely well ordered,¹⁴ which therefore excludes disorder as the dominant source of tunneling in this case. We find that the magnetic susceptibility is compatible with a perfect alignment (within less than 3°) of the anisotropy axes. In addition, the magnetic relaxation turns out to be faster in the disorder-free derivative than in Mn_{12} acetate. By a direct comparison of these data with the results of numerical simulations, we find an upper bound to the maximum orthorhombic parameter E induced by distortions in the latter compound.

Single crystals of Mn_{12} acetate and Mn_{12} -tBuAc were synthesized following published methods.^{14,15} Single crystals of optimum quality were selected and characterized using a four-circle x-ray diffractometer. Susceptibility data were measured on a $1 \times 0.4 \times 0.78$ mm³ Mn_{12} -tBuAc single crystal and a Mn_{12} acetate single crystal of approximate dimensions $0.85 \times 0.39 \times 0.14$ mm³. The results agree quantitatively, within the experimental uncertainties, with those obtained with other single crystals of similar quality. ac susceptibility data were measured between 0.05 and 236 Hz using a commercial superconducting quantum interference device magnetometer, equipped with the option of rotating the sample *in situ*. The relative accuracy of angular changes is better than 0.1° . The crystals were attached to the holder with apiezon N grease and the axis of rotation was approximately parallel to the (110) crystallographic axis. The contributions of the grease and the rotating platform were measured separately, under identical conditions, and subtracted from the data.

ac susceptibility data of Mn_{12} -tBuAc are shown in Fig. 1. We call ψ the angle between the c axis and the ac magnetic field. The striking difference between the susceptibility measured for the parallel and perpendicular orientations arises

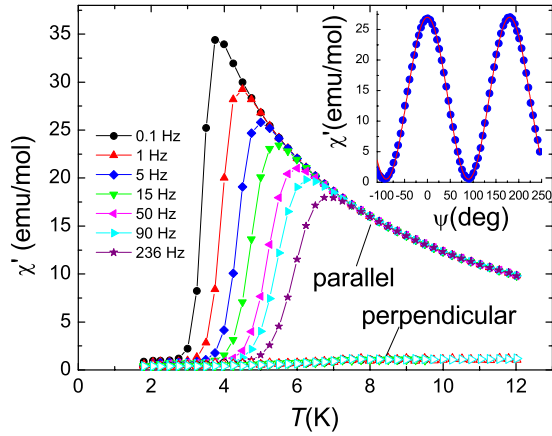


FIG. 1. (Color online) ac susceptibility data of a single crystal of Mn_{12} -tBuAc measured along and perpendicular to the crystallographic c axis. The inset shows the angular dependence of the susceptibility measured at $T=4.8$ K and for a frequency $\nu/2 = 1$ Hz (equilibrium).

from the strong magnetic anisotropy of these clusters. For an arbitrary orientation, the complex linear response of a (super)paramagnetic material with uniaxial anisotropy can be decomposed as

$$\chi = \chi_{\parallel} \cos^2 \psi + \chi_{\perp} \sin^2 \psi, \quad (1)$$

where χ_{\parallel} and χ_{\perp} are the parallel and perpendicular complex susceptibilities, respectively. Data measured at a fixed temperature $T=4.8$ K agree with the behavior predicted by Eq. (1), as it is shown by the inset of Fig. 1. The agreement shows the good quality of Mn_{12} -tBuAc as a reference sample.

Our study of the misalignment of the molecular anisotropy axes is entirely based on Eq. (1) and on the special properties of χ_{\parallel} and χ_{\perp} . The former depends on the frequency of the ac magnetic field because it reflects changes in the relative occupations of “spin-up” and “spin-down” states, which require flipping some spins across the anisotropy barrier. By contrast, χ_{\perp} is independent of frequency, as it mainly reflects the reversible tilt of the magnetic moments toward the transverse magnetic field. The frequency-dependent χ_{\parallel} can be described by a Cole-Cole function,¹⁶ which, together with Eq. (1), gives

$$\chi = \cos^2 \psi \frac{\chi_{\parallel,T}}{1 + (i\nu\tau)^{\beta}} + \sin^2 \psi \chi_{\perp,T}, \quad (2)$$

where $\chi_{\parallel,T} = N_A g^2 \mu_B^2 S^2 / k_B (T - \theta)$ and $\chi_{\perp,T} = N_A g^2 \mu_B^2 S / (2S - 1)D$ are the equilibrium (i.e., zero-frequency) limits of χ_{\parallel} and χ_{\perp} ,¹⁷ respectively, θ is the Weiss temperature, τ is the magnetic relaxation time, and β is a parameter that accounts for its distribution.

In Eq. (2), we have introduced the effect of orientational disorder by replacing $\cos^2 \psi$ and $\sin^2 \psi$ by their averages. Contrary to the magnetization, the zero-field susceptibility does not average out to zero in the case of randomly oriented anisotropy axes. The susceptibility provides then a direct method to determine their alignment in a given sample. In particular, the minimum of the frequency-dependent part of

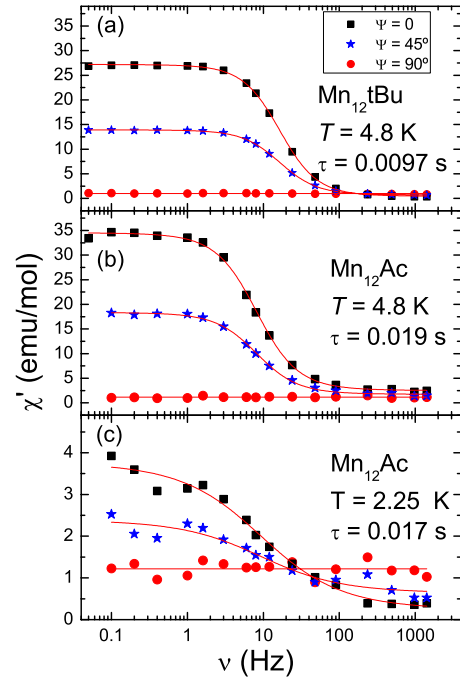


FIG. 2. (Color online) Frequency-dependent ac susceptibility of single crystals of (a) Mn_{12} -tBuAc and (b) and (c) Mn_{12} acetate. Solid lines are least-square fits of a Cole-Cole function Eq. (2) to the data, from which the relaxation time τ and the susceptibility drop $\Delta\chi$ between the low- and high-frequency limits are estimated.

the susceptibility the first term of Eq. (2) vanishes if, and only if, all anisotropy axes are perfectly aligned. Otherwise, there will always remain, at any orientation, some “contamination” of the parallel susceptibility. Notice that for sufficiently low temperatures, $\chi_{\parallel,T} \gg \chi_{\perp,T}$ making this effect noticeable even for small misalignments.

We can now compare the results obtained for the two Mn_{12} derivatives. Frequency-dependent susceptibility data measured at $T=4.8$ K and varying values of ψ are shown in Fig. 2 (a and b panels). For the disorder-free Mn_{12} -tBuAc, the minimum susceptibility, corresponding to $\psi=90^\circ$ (see the inset of Fig. 1) becomes indeed independent of frequency. This result confirms the good alignment of the molecular axes in this sample. Interestingly, the same behavior, within experimental uncertainties, is also observed for Mn_{12} acetate. In the latter sample, though, the high-frequency response at this temperature is dominated by the existence of “fast-relaxing” (FR) clusters, i.e., clusters having a weaker net magnetic anisotropy and therefore a much faster magnetic relaxation. To measure the frequency-dependent part of the FR component we decrease the temperature so that the susceptibility drop takes place within the experimental frequency “window.” In this way, the orientation of the two species can be investigated, independently of each other, in the same crystal.

For each orientation, we have determined the overall change $\Delta\chi = \chi_T - \chi_S$ of the in-phase susceptibility χ' between its equilibrium χ_T and high-frequency or adiabatic χ_S limits. According to Eq. (2), $\Delta\chi = \cos^2 \psi \chi_{\parallel,T}$. We plot this quantity in Fig. 3 as a function of angle for the standard Mn_{12} clusters in the two compounds as well as for the FR

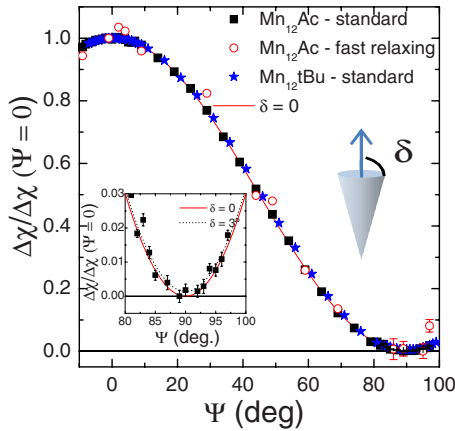


FIG. 3. (Color online) Angular dependence of $\Delta\chi$ (normalized by its value at $\psi=0$) for the slow and fast-relaxing species in the two Mn_{12} derivatives. The solid line represents the prediction for perfectly oriented anisotropy axes. The inset shows a magnification of the data measured for the standard Mn_{12} acetate clusters in the proximity of $\psi=90^\circ$. These data are compared with predictions for two configurations of the anisotropy axes.

clusters present in the acetate. It can be seen that $\Delta\chi$ agrees well with predictions for perfectly ordered anisotropy axes. The inset of Fig. 3 shows a magnification of the data measured for Mn_{12} acetate in the neighborhood of $\psi=90^\circ$. They are compared with a simulation made for a discrete set of spins having their anisotropy axes tilted by an angle δ and equally distributed on a cone centered around the c axis. Taking into account the experimental uncertainties, we find an upper bound for the easy axes misalignment of about 3° . Curiously enough, we find also a good alignment of the FR species along the c axis, although in this case the upper bound is of order 6° .

We next consider the effect that interstitial disorder has on the magnetic relaxation and tunneling rates. The relaxation rate has been determined, at each temperature, by fitting the frequency-dependent longitudinal susceptibility with Eq. (2). As it is already apparent from the data of Fig. 2, we find a faster relaxation for the Mn_{12} -tBuAc compound. The same is observed at all temperatures, as can be seen in Fig. 4.

The relaxation time obeys the Arrhenius law $\tau = \tau_0 \exp(U/k_B T)$ characteristic of a thermally activated process. We find $U=66(1)$ K and $\tau_0=2.3(5) \times 10^{-8}$ s for Mn_{12} acetate and $U=65(1)$ K and $\tau_0=1.3(5) \times 10^{-8}$ s for Mn_{12} -tBuAc.¹⁸ As we argue next, the slightly different magnetization dynamics in the two compounds can be accounted for rather well by taking into account the different strengths of dipolar interactions in the two crystal lattices. We have calculated the relaxation times by numerically solving a master equation²⁰ that includes phonon-induced transitions between eigenstates of the spin Hamiltonian

$$\mathcal{H} = -DS_z^2 + A_4S_z^4 + C(S_+^4 + S_-^4) + g\mu_B \mathbf{S} \cdot \mathbf{H}_{\text{dip}}. \quad (3)$$

The anisotropy parameters D , A_4 , and C are those allowed by the pure tetragonal symmetry of the molecular core. They have been determined by different spectroscopic techniques.^{21–24} For the two compounds, and within the experi-

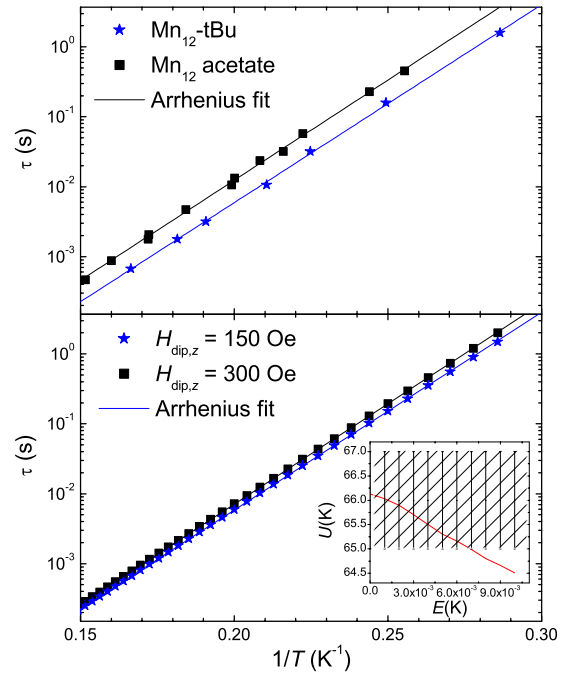


FIG. 4. (Color online) Top: magnetic relaxation time of Mn_{12} -tBuAc and Mn_{12} acetate. Solid lines are least-square Arrhenius fits giving activation energies $U=65(1)$ K for the former compound and $U=66(1)$ K for the latter. Bottom: relaxation time calculated with the model described in Ref. 20 and the Hamiltonian parameters given in the text. Results obtained for two values of the dipolar bias field are shown. The activation energies are $U=65.1$ K for $H_{\text{dip},z}=150$ Oe and $U=66.1$ K for $H_{\text{dip},z}=300$ Oe. The inset shows the dependence of U , calculated for $H_{\text{dip},z}=300$ Oe, on the orthorhombic parameter E . The shadowed area represents experimentally acceptable values for Mn_{12} acetate.

mental errors, $D=0.56$ K, $A_4=-1.1 \times 10^{-3}$ K, and $C=-2.2 \times 10^{-5}$ K, i.e., they have the same total, or classical, anisotropy energy barrier $U_{\text{cl}}=DS^2-A_4S^4$. The last term in Eq. (3) describes the effect of dipole-dipole interactions via an effective magnetic field H_{dip} . At zero field, when molecular spins point randomly either up or down, interactions give rise to a nearly Gaussian distribution of dipolar fields along the anisotropy axis (bias field) and perpendicular to it.²⁵ As a first approximation,²⁶ we estimate a typical bias dipolar field from the relationship $2H_{\text{dip},z}g\mu_B S = k_B\theta$, where θ is the Weiss temperature, determined from the fit of the equilibrium susceptibility, that is, of χ' measured above the blocking temperature.¹³ Inserting $\theta=0.4$ K for Mn_{12} -tBuAc and $\theta=0.8$ K for Mn_{12} acetate gives $H_{\text{dip},z}=150$ and 300 Oe, respectively. We have also introduced a transverse component $H_{\text{dip},x}=\sqrt{2}H_{\text{dip},z}$ which enables tunneling between any pair of degenerate spin states.²⁰

Calculated results are shown in the bottom panel of Fig. 4. Relaxation is indeed faster for the sample with weaker interactions, as we observe experimentally. The reason is that the dipolar bias energetically “detunes” spin states with opposite orientations, then blocking the tunneling process. Clearly, there is no need to include any additional off-diagonal term in the acetate compound, arising from interstitial disorder. As the inset of Fig. 4 shows, such a term promotes tunneling and

would therefore lower the activation energy of Mn₁₂ acetate with respect to that of Mn₁₂-tBuAc, i.e., exactly the opposite as observed. Still, we can find an upper bound for the maximum orthorhombic parameter E compatible with the experimental results. We find $E = 6 \times 10^{-3}$ K. This upper bound is somewhat smaller than $E = 8.6(1.4) \times 10^{-3}$ K, estimated from inelastic neutron-scattering experiments²³ and it is also lower, although compatible with, upper bounds estimated from ESR (Ref. 10) ($E = 1.15 \times 10^{-2}$ K) and Landau-Zener magnetic relaxation²⁸ ($E = 1.0 \times 10^{-2}$ K) experiments.

Concluding, susceptibility data measured on two Mn₁₂ derivatives, with different degree of interstitial disorder, are compatible with a perfect alignment of the anisotropy axes. In addition, the magnetic relaxation of the axially symmetric Mn₁₂-tBuAc is faster than the relaxation of Mn₁₂ acetate.

Although the influence of disorder cannot be excluded, as it has been put in evidence by recent experiments,²⁹ the present results question it as the *dominant* origin of quantum tunneling in Mn₁₂ acetate. In other words, it is not a necessary ingredient for the existence of this quantum phenomenon at zero field. Most of the observed features are, in fact, well accounted for by a model including the off-diagonal anisotropy terms allowed by the pure molecular symmetry and Zeeman terms that describe the effect of dipolar magnetic interactions.

This work has been partly funded by grants MOLCHIP and Molecular Nanoscience from the Spanish MICINN, and NABISUP from DGA. We also acknowledge support from the European Network of Excellence MAGMANet.

*Corresponding author. uis@unizar.es

¹D. Gatteschi, R. Sessoli, and J. Villain, *Molecular Nanomagnets* (Oxford University Press, Oxford, 2006).

²R. Sessoli, D. Gatteschi, A. Caneschi, and M. A. Novak, *Nature* (London) **365**, 141 (1993).

³R. Sessoli, H.-K. Tsai, A. R. Schake, S. Wang, J. B. Vincent, K. Folting, D. Gatteschi, G. Christou, and D. N. Hendrickson, *J. Am. Chem. Soc.* **115**, 1804 (1993).

⁴C. Paulsen, J.-G. Park, B. Barbara, R. Sessoli, and A. Caneschi, *J. Magn. Magn. Mater.* **140-144**, 1891 (1995).

⁵J. R. Friedman, M. P. Sarachik, J. Tejada, and R. Ziolo, *Phys. Rev. Lett.* **76**, 3830 (1996).

⁶J. M. Hernández, X. X. Zhang, F. Luis, J. Bartolomé, J. Tejada, and R. Ziolo, *Europhys. Lett.* **35**, 301 (1996).

⁷L. Thomas, F. Lioni, R. Ballou, D. Gatteschi, R. Sessoli, and B. Barbara, *Nature* (London) **383**, 145 (1996).

⁸E. M. Chudnovsky and D. A. Garanin, *Phys. Rev. Lett.* **87**, 187203 (2001).

⁹A. Cornia, R. Sessoli, L. Sorace, D. Gatteschi, A. L. Barra, and C. Daugebonne, *Phys. Rev. Lett.* **89**, 257201 (2002).

¹⁰S. Takahashi, R. S. Edwards, J. M. North, S. Hill, and N. S. Dalal, *Phys. Rev. B* **70**, 094429 (2004).

¹¹E. del Barco, A. D. Kent, N. E. Chakov, L. N. Zakharov, A. L. Rheingold, D. N. Hendrickson, and G. Christou, *Phys. Rev. B* **69**, 020411(R) (2004).

¹²W. Wernsdorfer, N. E. Chakov, and G. Christou, *Phys. Rev. B* **70**, 132413 (2004).

¹³F. Luis, J. Campo, J. Gómez, G. J. McIntyre, J. Luzón, and D. Ruiz-Molina, *Phys. Rev. Lett.* **95**, 227202 (2005).

¹⁴W. Wernsdorfer, M. Murugesu, and G. Christou, *Phys. Rev. Lett.* **96**, 057208 (2006).

¹⁵T. Lis, *Acta Crystallogr., Sect. B: Struct. Crystallogr. Cryst. Chem.* **36**, 2042 (1980).

¹⁶K. S. Cole and R. H. Cole, *J. Chem. Phys.* **9**, 341 (1941).

¹⁷J. L. García-Palacios, J. B. Gong, and F. Luis, *J. Phys.: Condens. Matter* **21**, 456006 (2009).

¹⁸The effective activation energy can slightly depend on temperature (Ref. 19). For Mn₁₂ acetate, we observe this effect when

$1/T = 0.16 \text{ K}^{-1}$. For this reason, we have compared fits done within the temperature region $0.16 \text{ K}^{-1} < 1/T < 0.29 \text{ K}^{-1}$.

¹⁹C. Lampropoulos, S. O. Hill, and G. Christou, *ChemPhysChem* **10**, 2397 (2009).

²⁰F. Luis, J. Bartolomé, and J. F. Fernández, *Phys. Rev. B* **57**, 505 (1998).

²¹A.-L. Barra, D. Gatteschi, and R. Sessoli, *Phys. Rev. B* **56**, 8192 (1997).

²²I. Mirebeau, M. Hennion, H. Casalta, H. Andres, H. U. Güdel, A. V. Irodova, and A. Caneschi, *Phys. Rev. Lett.* **83**, 628 (1999).

²³R. Bircher, G. Chaboussant, A. Sieber, H. U. Güdel, and H. Mutka, *Phys. Rev. B* **70**, 212413 (2004).

²⁴A.-L. Barra, A. Caneschi, A. Cornia, D. Gatteschi, L. Gorini, L.-P. Heiniger, R. Sessoli, and L. Sorace, *J. Am. Chem. Soc.* **129**, 10754 (2007).

²⁵J. H. Van Vleck, *Phys. Rev.* **57**, 426 (1940).

²⁶In a mean-field approximation, $k_B \theta = H_m g \mu_B S$ (Ref. 27), where $H_m = \langle M_s \rangle$ is the mean field in a magnetically saturated state and M_s is the saturation magnetization. The approximation used is therefore equivalent to setting the typical dipolar field in the unpolarized state as equal to one half of the maximum H_m . The ratio between the interaction fields of the two compounds (two times larger for the acetate) determined from θ agrees, in fact, with the ratio 1.9 of their saturation magnetizations, which arises from the smaller unit-cell volume of Mn₁₂ acetate (3.72 nm^3) as compared with that of Mn₁₂-tBuAc (7.06 nm^3). The same applies to the dipolar fields created by the two nearest-neighbor spins along the anisotropy axis, which amounts to 388 Oe for Mn₁₂ acetate and 200 Oe for Mn₁₂-tBuAc.

²⁷M. R. Roser and L. R. Corruccini, *Phys. Rev. Lett.* **65**, 1064 (1990).

²⁸E. del Barco, A. D. Kent, E. M. Rumberger, D. N. Hendrickson, and G. Christou, *Phys. Rev. Lett.* **91**, 047203 (2003).

²⁹G. Redler, C. Lampropoulos, S. Datta, C. Koo, T. C. Stamatatos, N. E. Chakov, G. Christou, and S. Hill, *Phys. Rev. B* **80**, 094408 (2009).